

Parallel optical nanolithography using nanoscale bowtie aperture array

Sreemanth M.V. Uppuluri, Edward C. Kinzel, Yan Li, and Xianfan Xu*

*School of Mechanical Engineering and Birck Nanotechnology Center, Purdue University,
West Lafayette, IN 47906, USA*

**xxu@purdue.edu*

Abstract: We report results of parallel optical nanolithography using nanoscale bowtie aperture array. These nanoscale bowtie aperture arrays are used to focus a laser beam into multiple nanoscale light spots for parallel nano-lithography. Our work employed a frequency-tripled diode-pumped solid state (DPSS) laser ($\lambda = 355$ nm) and Shipley S1805 photoresist. An interference-based optical alignment system was employed to position the bowtie aperture arrays with the photoresist surface. Nanoscale direct-writing of sub-100nm features in photoresist in parallel is demonstrated.

©2010 Optical Society of America

OCIS codes: (110.4235) Nanolithography; (220.4241) Nanostructure fabrication; (120.3180) Interferometry.

References and links

1. S. Sun, and G. J. Leggett, "Matching the resolution of electron beam lithography by scanning near-field photolithography," *Nano Lett.* **4**(8), 1381–1384 (2004).
2. M. M. Alkaisi, R. J. Blaikie, S. J. McNab, R. Cheung, and D. R. S. Cumming, "Sub-diffraction-limited patterning using evanescent near-field optical lithography," *Appl. Phys. Lett.* **75**(22), 3560–3562 (1999).
3. Z. W. Liu, Q. H. Wei, and X. Zhang, "Surface plasmon interference nanolithography," *Nano Lett.* **5**(5), 957–961 (2005).
4. X. Shi, and L. Hesselink, "Mechanisms for enhancing power throughput from planar nano-apertures for near-field optical data storage," *Jpn. J. Appl. Phys.* **41**(Part 1, No. 3B), 1632–1635 (2002).
5. K. Şendur, W. Challener, and C. Peng, "Ridge waveguide as a near field aperture for high density data storage," *J. Appl. Phys.* **96**(5), 2743–2752 (2004).
6. E. X. Jin, and X. Xu, "Finite difference time domain studies on optical transmission through planar nano-apertures in a metal film," *Jpn. J. Appl. Phys.* **43**(1), 407–417 (2004).
7. F. Chen, A. Itagi, J. A. Bain, D. D. Stancil, T. E. Schlesinger, L. Stebounova, G. C. Walker, and B. B. Akhremitchev, "Imaging of optical field confinement in ridge waveguides fabricated on very-small-aperture laser," *Appl. Phys. Lett.* **83**(16), 3245–3247 (2003).
8. L. Wang, S. M. V. Uppuluri, E. X. Jin, and X. Xu, "Nanolithography using high transmission nanoscale bowtie apertures," *Nano Lett.* **6**(3), 361–364 (2006).
9. N. Murphy-DuBay, L. Wang, E. C. Kinzel, S. M. V. Uppuluri, and X. Xu, "Nanopatterning using NSOM probes integrated with high transmission nanoscale bowtie aperture," *Opt. Express* **16**(4), 2584–2589 (2008).
10. Y. Kim, S. Kim, H. Jung, E. Lee, and J. W. Hahn, "Plasmonic nano lithography with a high scan speed contact probe," *Opt. Express* **17**(22), 19476–19485 (2009).
11. W. Srituravanich, L. Pan, Y. Wang, C. Sun, D. B. Bogy, and X. Zhang, "Flying plasmonic lens in the near field for high-speed nanolithography," *Nat. Nanotechnol.* **3**(12), 733–737 (2008).
12. E. X. Jin, and X. Xu, "Obtaining super resolution light spot using surface plasmon assisted sharp ridge nano-aperture," *Appl. Phys. Lett.* **86**(11), 111106–111108 (2005).
13. Solvay Solexis Inc, "Fomblin Lubes – PFPE lubricants",
<http://www.solvaysolexis.com/static/wma/pdf/1/4/9/7/3/BR%20FOMB%20Lubes%20LD.pdf>.
14. Remcom Inc., FDTD Commercial Software Package, Version XFDTD 6.3.
15. H. Gai, J. Wang, and Q. Tian, "Modified Debye model parameters of metals applicable for broadband calculations," *Appl. Opt.* **46**(12), 2229–2233 (2007).
16. P. B. Johnson, and R. W. Christy, "Optical constants of transition metals: Ti, V, Cr, Mn, Fe, Co, Ni and Pd," *Phys. Rev. B* **9**(12), 5056–5070 (1974).
17. E. D. Palik, *Handbook of Optical Constants of Solids* (Academic Press, 1985).
18. M. Despont, J. Brugger, U. Dürig, W. Häberle, M. Lutwyche, H. Rothuizen, R. Stutz, R. Widmer, G. Binnig, H. Rohrer, and P. Vettiger, "VLSI-NEMS chip for parallel AFM data storage," *Sens. Actuators* **80**(2), 100–107 (2000).

1. Introduction

Nano-optics-based lithography has the potential to be a low-cost alternative to other nanofabrication techniques such as e-beam lithography. Many processes have been demonstrated towards this end, including near-field optical microscopy (NSOM)-based nanolithography [1], evanescent near-field optical lithography [2], and surface-plasmon interference nanolithography [3]. Ridge nanoscale apertures of different shapes (C, H, bowtie) have been shown to have a potential for optical nano-patterning via simulations [4–6] and also experimental demonstration [7–10]. Figure 1 shows the schematic of a bowtie-shaped ridge aperture. The unique property of ridge apertures enabling their application in nanolithography is that these apertures support a propagating TE_{01} mode when the incident laser light is polarized across the gap. The energy of this mode is concentrated in the gap region and thus a nanoscale light source is produced. The resolution of the light spot produced by these apertures is limited only by the fabrication capability of producing a small gap in these apertures. The radiation on the exit-plane of these apertures is however concentrated to within a small distance, of the order of tens of nanometers from the exit-plane, beyond which the light-spot increases significantly in size and decreases in intensity [6]. Thus using these apertures for nanolithography and nano-patterning necessitates intimate contact between the aperture exit-plane and the photoresist surface or accurate control of the separation distance to within a few nanometers. These have been accomplished in different ways including allowing the mask to ‘sit’ on the photoresist surface [8], using a closed-loop feedback mechanism [9], applying normal force to maintain contact [10], and using air-pressure to levitate the mask to a small height (\sim nm), similar to a computer hard-drive mechanism [11]. All the previous work dealing with ‘writing’ patterns is however limited to using a single source.

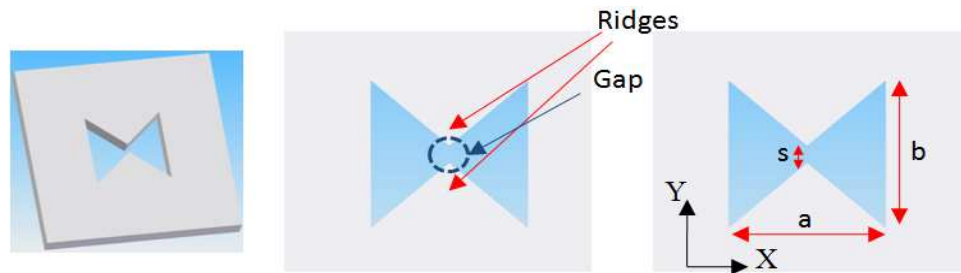


Fig. 1. Bowtie-shaped ridge aperture.

In this work we describe using a nanoscale bowtie aperture array for parallel nanolithography. In addition to the optical issues related to the nanoscale bowtie aperture, we also report other manufacturability considerations such as reducing the friction between the metal film and the photoresist surface. We present an optical interference-based alignment system to establish intimate contact between an array of apertures and the photoresist surface with minimum friction between the two surfaces, thus facilitating parallel nano direct-writing.

2. Experiment setup

Figure 2 shows a schematic of the experiment setup. During the nanolithography process the mask containing the bowtie aperture array is exposed to a frequency tripled diode-pumped solid state (DPSS) UV laser beam ($\lambda = 355$ nm) while the substrate is scanned using a piezoelectric stage to create patterns. The laser beam is expanded; therefore all bowtie apertures are exposed uniformly. The laser power intensity used is around 12.3 mW/cm^2 . During the experiment the mask is loaded onto a two-axis tilt stage whereas the photoresist sample is placed on top a high precision piezoelectric stage. The mask and photoresist surfaces are then aligned to a high degree of parallelism using an interferometer system which will be described later. The mask is then moved into contact with the photoresist surface. This minimizes the friction between the mask and the photoresist that allows the mask and the

photoresist to scan relative to each other to create patterns without damaging the mask or the photoresist.

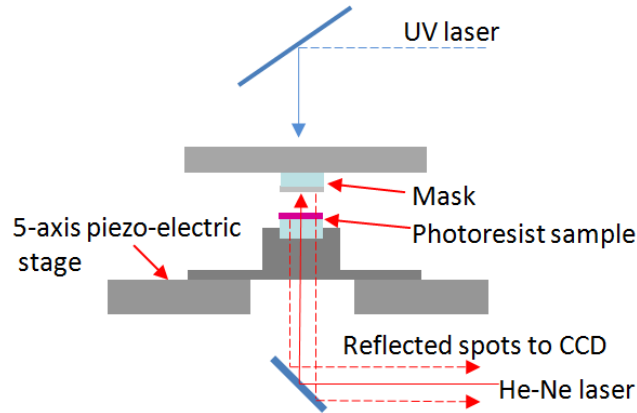


Fig. 2. Schematic of experiment setup.

The choice of the metal film for fabricating bowtie apertures is also important from the standpoint of aperture performance [6,12] and from the point of view of obtaining smooth films for maintaining a close contact between the aperture array and the photoresist surface. In the past, the behavior of ridge apertures is studied extensively for aluminum films due to high reflectivity and small skin-depth of aluminum in the visible and UV wavelength regime [8,9]. One of the main drawbacks of using aluminum for nano-aperture based lithography is the high friction coefficient between the bare aluminum film and the photoresist surface. Also, commonly available lubricant films [13] are incompatible with aluminum films. In addition, obtaining aluminum films with surface roughness better than 1 nm has been found to be a non-trivial task [10]. In this work we choose thermal PVD deposited chromium films which are shown as a viable thin-film material for parallel nano-lithography so far as creating high quality film is concerned. The optical performance of the apertures made in chromium is shown to be comparable with those in aluminum as is discussed next.

3. Numerical simulations

We used finite-difference-time-domain simulation software [14] to numerically design the bowtie apertures. The Modified Debye model [15] as shown in Eq. (1) is used to simulate the permittivity ($\tilde{\epsilon}$) values of the metal films.

$$\tilde{\epsilon} = \epsilon_{\infty} + \frac{\epsilon_s - \epsilon_{\infty}}{1 + j\omega\tau} + \frac{\sigma}{j\omega\epsilon_0}. \quad (1)$$

At the process wavelength of $\lambda = 355\text{nm}$, the material model parameters are $\epsilon_s = -23.591$, $\epsilon_{\infty} = 8.785$, $\tau = 2.3956 \times 10^{-16}\text{ s}$, $\sigma = 1.19662 \times 10^6\text{ S/m}$ for chromium and $\epsilon_s = -595$, $\epsilon_{\infty} = 1.01$, $\tau = 1.03 \times 10^{-15}\text{ s}$, $\sigma = 5.1235 \times 10^6\text{ S/m}$ for aluminum [16,17]. The simulation model consists of the metal film (Cr or Al) of thickness = 125 nm on top of a quartz substrate ($n = 1.5646 @ 355\text{ nm}$). We chose a thickness of 125 nm since it is sufficient to screen background radiation. The photoresist surface (Shipley S1805, $n = 1.7433 @ 355\text{ nm}$) is placed at varying distances from the aperture exit-plane, and the effect of the separation distance between the mask and the photoresist on the obtainable resolution is studied, considering the existence of the lubricant film (5 - 10 nm) and also that a small separation distance between the aperture and the mask may exist during experiments. The bowtie aperture is excited by an incident plane wave polarized across the gap of the aperture. The outline dimensions of the bowtie aperture are $a = b = 170\text{ nm}$ with a gap, $s = 25\text{ nm}$ (see Fig. 1). These dimensions (a and b) are chosen

from numerical computation optimizations so that the higher order modes are not excited in the bowtie aperture and the smallest obtainable spot size may be realized. The gap size is chosen based on the fabrication resolution that can be achieved using an FIB machine at Purdue University.

Figures 3(a) and 3(b) show the maximum electric field distribution in the E and H-planes of bowtie apertures milled in aluminum and chromium films, respectively. For the results shown in Fig. 3, a gap of 10 nm is used between the metal film and the photoresist surface. As seen from the figure the magnitude of the electric fields and the corresponding spot sizes are very close for the aluminum and chromium films.

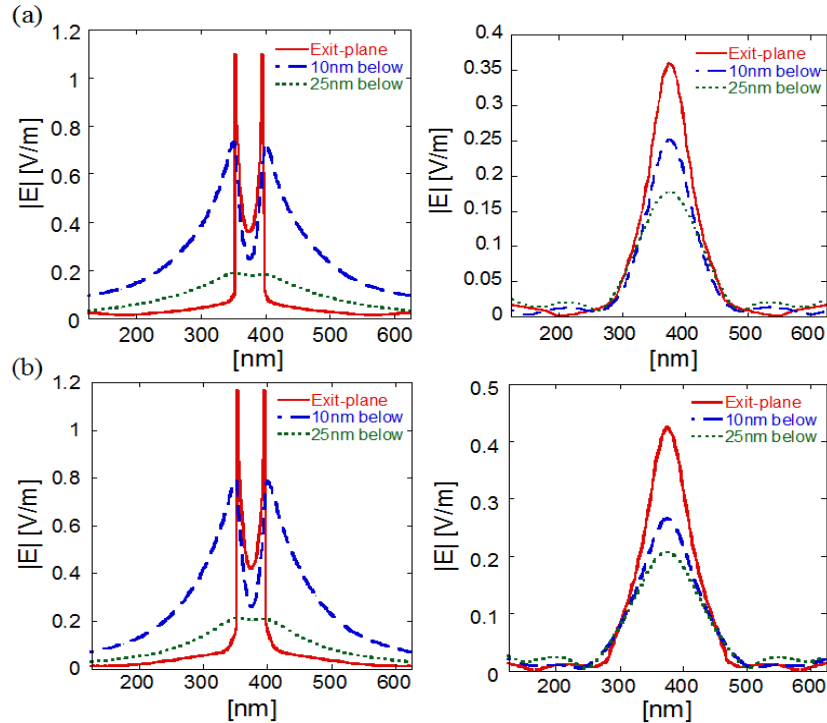


Fig. 3. (a) Electric field distributions in the E and H planes for Aluminum bowtie aperture, (b) Electric field distributions in the E and H planes for Chromium bowtie aperture.

4. Experimental details

We used optically flat ($\lambda/20$ @ $\lambda = 633$ nm) quartz substrates for preparing masks as well as photoresist samples. The metal films are prepared by thermal evaporation of chromium on quartz substrates at a deposition rate of around 0.5 \AA/s . Figures 4(a) and 4(b) show respectively the SEM and AFM images of the metal film. The roughness measured using atomic force microscopy (AFM) is less than 1 nm over an area of $25 \mu\text{m}^2$. Apertures are defined in the metal film using FIB milling (FEI Nova 200 Dual Beam FIB/SEM), with an outline dimension of $170 \text{ nm} \times 170 \text{ nm}$ (obtained from numerical simulation as discussed above) and a gap size of 25 nm. The Cr film is then spin-coated with a 5-10 nm lubricant Fomblin Z-Dol. The Z-Dol lubricant film is found to decrease the friction coefficient by a factor of 3 and thus facilitates smoother motion of the mask relative to the photoresist surface. The photoresist film (diluted S1805, at a dilution ratio of 1:6 in thinner type P) is spin-coated on optically-flat quartz substrates. The RMS roughness of the photoresist films as measured using atomic force microscopy is around 0.3 nm.

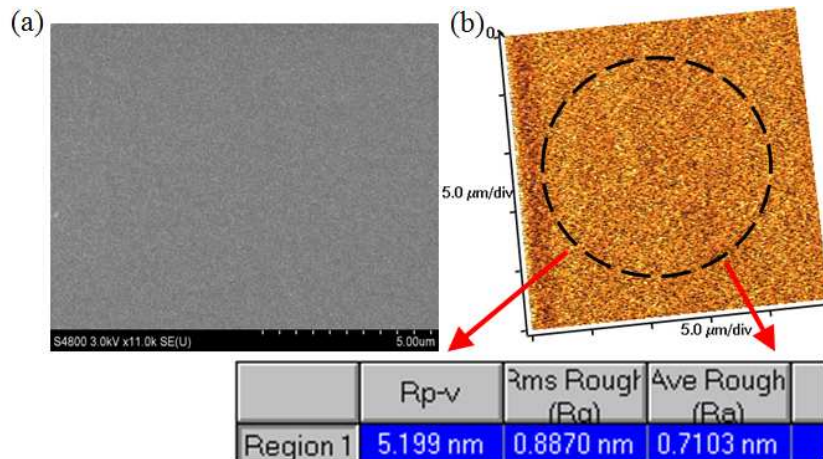


Fig. 4. Ultra-smooth chromium film prepared by the thermal PVD process. (a) SEM image, (b) AFM topography image.

An important step in using the bowtie aperture array for nanolithography is aligning the mask containing the bowtie aperture array with the photoresist-coated substrate. The goal is to achieve high degree of parallelism between the mask and the photoresist surfaces as they are brought to contact, thus reducing friction during their relative motion. To accomplish this task we designed an optical interference-based alignment system. The tilt between the two surfaces is initially adjusted by detecting the reflected laser spots from the mask and photoresist surfaces using a quadrant photodiode (SPOT-9DMI, Optoelectronics Inc). By nulling the signals generated by each reflected laser spot to within the measurement sensitivity, we achieved a planar alignment in the order of 1 mrad between the two surfaces. Further alignment is then achieved by using the fringes produced by the interference of the two reflected spots. The width and the density of these fringes is a function of the relative tilt between the two surfaces. By adjusting the tilt of the photoresist surface using a high-precision piezoelectric stage the observed interference fringes can be reduced to zero over the entire cross-section of the He-Ne laser spot. This ensures a planar parallelity of within 0.1 mrad. In an area of about $55 \mu\text{m} \times 55 \mu\text{m}$ where the bowtie array is fabricated, this implies a planar alignment of about 5.5 nm in the x- and y-directions. Figure 5(a) shows the fringe pattern observed experimentally for varying degrees of tilt between the mask and photoresist surfaces. In the figure the horizontally inclined fringes correspond to those obtained from interference of the reflected spots from the mask and photoresist surfaces whereas the vertically inclined fringes are caused by a filter that is used to attenuate the brightness of the He-Ne laser. Thus the vertical fringes have no bearing with the tilt misalignment between the two surfaces. Figure 5(b) shows the fringe pattern from MATLAB simulations based on geometric optics and interference theory. As seen from the figures the number of fringes and the fringe density observed in experiment follow closely those predicted from MATLAB simulations. As the present alignment system involves planar alignment using interference fringes formed from the reflected spots from the mask and photoresist surfaces, we believe that the alignment system does not impose any constraint on the maximum size of the bowtie aperture array that can be used for parallel nanolithography. The largest patterning area on the mask that is aligned to parallelity using the present interference system has been around 1.96 mm^2 . To improve the alignment accuracy for even larger patterning areas ($> 1 \text{ cm}^2$), a possibility is using multiple He-Ne laser beams at different locations and adjusting the tilt between the mask and photoresist surfaces to reduce the number of interference fringes at all the locations simultaneously to zero.

In comparison to other parallel nano-patterning technologies such as AFM based millipede system [18], we believe that the present system offers a simpler design for parallel

nanolithography. The main limitation of the present system is that it requires the photoresist coated substrate to be transparent or semi-transparent to the He-Ne laser beam for allowing the laser to pass through it. Thus the present alignment system needs to be modified for use with photoresist coated silicon substrates.

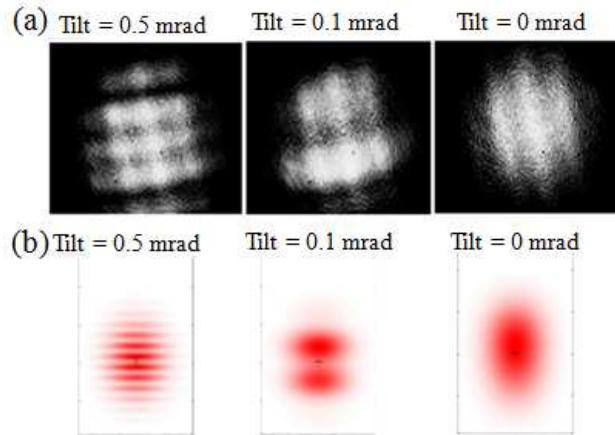


Fig. 5. Interference fringes for varying degrees of tilt between the mask and photoresist surfaces. (a) Measured, (b) MATLAB simulations.

5. Experimental results

Figure 6(a) shows a plot of line widths produced in photoresist for varying scan speeds and Fig. 6(b) shows the corresponding plot of line depths in the photoresist. As can be seen the line width and depth decrease with increasing scan speeds. As mentioned earlier, expanding the laser beam to expose an array of bowtie apertures causes significant reduction in the laser power intensity, hence a relatively low laser intensity is used and the maximum scan speed in our experiments is around $1 \mu\text{m/s}$. Beyond this value the lines became too shallow and irregular. The speed of nanopatterning may be improved by using a laser beam in conjunction with other optical elements such as a diffractive optical element combined with a microlens array such as a digital micro-mirror device (DMD), which allows exposing individual bowtie apertures at fluence levels greater than that in the present system. Using such a system allows switching ON/OFF bowtie apertures in the array selectively and thus offers a versatile system for writing more intricate patterns.

The expected line-widths based on FDTD simulations are shown in Fig. 6(c) for a separation distance of 10 nm between the mask and photoresist surfaces. These line widths are based on threshold dose calculations (for a measured resist threshold dose of 5 mJ/cm^2) and the results are found to be close to those obtained from the experiment. The differences in the exact line widths between the simulations and the experiments could be attributed to ambiguities in the nature of the exact distance between the bowtie aperture and the photoresist surface. The shape of the bowtie aperture obtained from FIB milling could also be different from that used in the simulations. Figure 6(d) shows an AFM image of a line of about 90 nm wide for a scan speed of $0.5 \mu\text{m/s}$. The narrowest line width obtained is about 60 nm and is shown in Fig. 6(e). However, as is evident, for such narrow line widths, the edge becomes irregular and not repeatable. The two hot-spots from the bowtie aperture affect the nanopatterning resolution during scanning in the x-direction (the x-axis direction as indicated in Fig. 1), but not the other, which was confirmed in our experiments (all results shown here correspond to scanning along the y-direction, the direction as indicated in Fig. 1). Thus for nanopatterning involving scanning in both x and y-directions it is preferable to use a single-tip nanoaperture instead of a bowtie (two-tip) aperture.

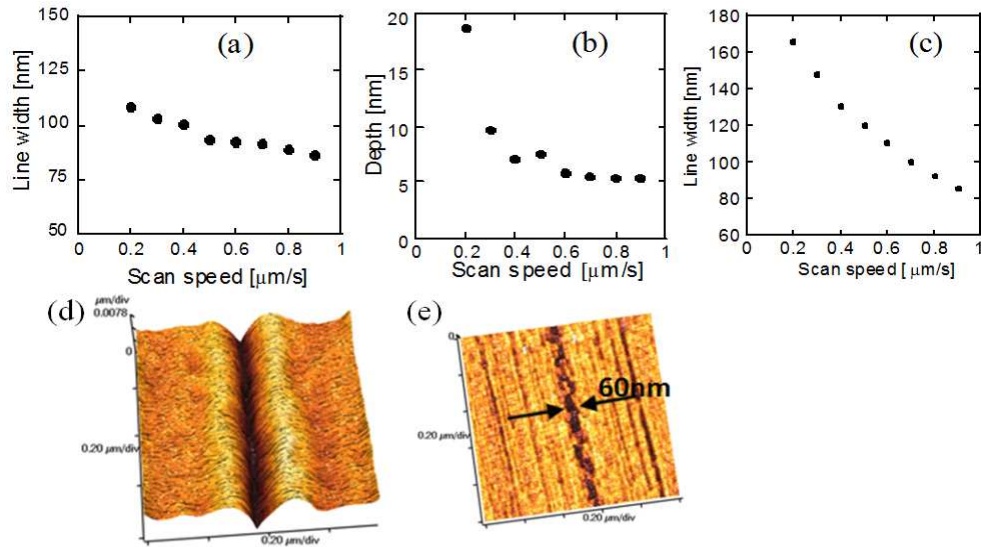


Fig. 6. Lines generated at different speeds – 0.2, 0.3, 0.4, 0.5, 0.6, 0.7, 0.8, 0.9 $\mu\text{m/s}$. (a) width of the lines, (b) depth of the lines, (c) XFDTD prediction of line widths, (d) AFM image of line width ~ 90 nm, (e) AFM image of smallest line width of about 60 nm.

Figure 7 demonstrates patterning using an array of bowtie apertures in parallel. Figure 7(a) shows an SEM image of a 2×2 bowtie array and Fig. 7(b) shows the AFM image of the patterned photoresist film (letters BNC as in Birck Nanotechnology Center of Purdue University). The line width obtained during this experiment is around 85-90 nm for a scan speed = 0.5 $\mu\text{m/s}$.

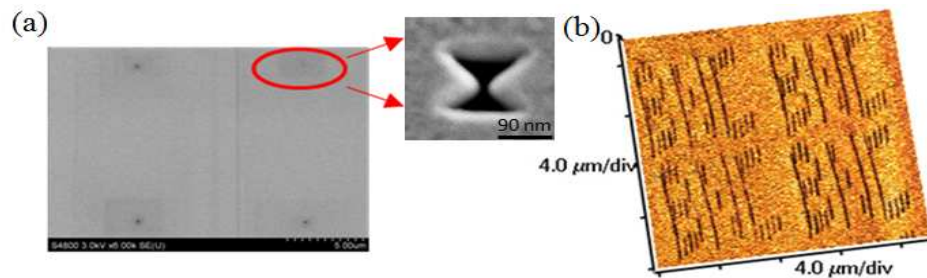


Fig. 7. Parallel writing using a 2×2 array of Bowtie apertures. (a) SEM image of the mask, (b) AFM image of patterns produced in the photoresist.

6. Conclusions

In conclusion, we describe a nanoscale lithography system using light spots produced by a bowtie aperture array. It includes an interference-based optical alignment system for aligning the array of nanoscale bowtie apertures to a high degree of parallelity with a photoresist coated substrate. Our experiments achieved parallel patterning, with a resolution in the order of 85-90 nm with high degree of repeatability.

Acknowledgements

Support for this work provided by the National Science Foundation (NSF) (DMI-0707817, DMI-0456809) and the Defense Advanced Research Project Agency (DARPA) grant N66001-08-1-2037. Program Manager Dr. Thomas Kenny is gratefully acknowledged. The authors also thank Luis M. Traverso for his help with the experiments.